

Initiation of fatigue cracks in AZ91 Mg alloy processed by ECAP

S Fintová¹ and L Kunz²

¹ Brno University of Technology, CEITEC BUT – Central European Institute of Technology, Technická 3058/10, 616 00 Brno, CZ, e-mail: stanislava.fintova@ceitec.vutbr.cz

² Institute of Physics of Materials AS CR, Žitkova 22, 616 62 Brno, CZ, e-mail: kunz@ipm.cz

Abstract. Mechanism of fatigue crack initiation was investigated in ultrafine-grained (UFG) magnesium alloy AZ91 processed by equal channel angular pressing (ECAP). Fatigue behaviour of UFG material was compared to the behaviour of material in an initial as-cast state. Focused ion beam technique (FIB) was applied to reveal the surface relief and early fatigue cracks. Two substantially different mechanisms of crack initiation were observed in UFG structure, which can be characterized as bimodal even after 6 ECAP passes by route Bc. The bimodality consists in a coexistence of very fine grained areas with higher content of Mg₁₇Al₁₂ particles and areas exhibiting somewhat larger grains and lower density of particles. The fatigue cracks which initiate in areas of larger grains are related to the cyclic slip bands; this initiation mechanism is similar to that observed in cast alloy. The second initiation mechanism is related to the grain boundary cracking which takes place predominantly in the fine grained areas.

1. Introduction

Magnesium alloys are used especially because of their low weight but still good mechanical properties. Based on the chemical composition and resulting microstructure, different ratio among individual material properties can be reached [1 – 7].

Though there is a relatively extensive knowledge on relation of microstructure and mechanical properties of Mg alloys, methods of further improvement of the mechanical properties is still a discussed issue, permanently activated by engineering practice and industrial demands. One of the ways how to improve mechanical properties is application of severe plastic deformation (SPD). Equal channel angular pressing (ECAP) is one of the most studied and explored techniques. ECAP treatment performed at elevated temperatures can improve tensile properties of magnesium alloys, corrosion properties and also fatigue strength [8, 9]. On the other hand also lowering of tensile and fatigue strength were reported for wrought Mg alloys processed by ECAP [10, 11, 12]. Elevated temperatures under which the SPD is applied are necessary for activation of sufficient amount of slip systems in magnesium hcp crystallographic lattice. It has been shown that suitable heat treatment of the initial cast alloy before ECAP promotes formation of more homogenous structure and the ECAP refines than the structure more effectively. When a proper heat treatment is applied before ECAP, only 2 passes through ECAP die are sufficient to refine the structure and significantly improve the yield stress and tensile strength. Following passes through ECAP die homogenize the structure whereas the influence on mechanical properties of treated material is weak [5, 7, 8].

AZ91 magnesium alloy is one of the most often used magnesium alloys from AZ group. It contains relatively high volume of alloying elements; high volume of Al results in larger amount of Mg₁₇Al₁₂ intermetallic particles, which can be exploited in material hardening due to the treatment by ECAP [5]. ECAP process rises the yield stress ($\sigma_{0.2}$) and ultimate tensile strength (σ_{UTS}) (almost 100 % improvement), and, particularly, improves the ductility (A) (almost 500 % improvement) due to the substantial grain refinement [5, 7, 13].

The AZ91 alloy is primarily intended and used for fabrication of cast components. The fatigue behaviour of AZ91 in cast state was examined in [4, 14]. It has been shown that the endurance limit is of about 80 MPa. Wolf et al. [4] studied the fatigue behavior and the



mechanism of fatigue crack initiation and growth. They reported that the initiation of fatigue cracks takes place due to localization of the cyclic plastic deformation in slip bands which are formed in solid solution areas. Fatigue cracks initiate at the surface micro-relief at in-/extrusions and on interfaces between brittle $Mg_{17}Al_{12}$ intermetallic particles and ductile solid solution matrix. Also an $Mg_{17}Al_{12}$ intermetallic particle cracking was observed. The authors draw also the attention to the role of pores present in the material which can be sites of fatigue crack initiation.

The studies dealing with fatigue behaviour, crack initiation and growth in ECAPed AZ91 magnesium alloy are very rare. That is why this study was focused on the experimental determination of the S-N curve, investigation of mechanisms of fatigue crack initiation in UFG AZ91 processed by ECAP and comparison with the behaviour of the as-cast state.

2. Material and experiments

AZ91 magnesium alloy with chemical composition given in Table 1 was investigated. Cast billets were used with no preliminary heat treatment for ECAP. The processing temperature $300^{\circ}C$ was sufficient to perform the severe plastic deformation without cracking. Bc route was applied and the intersecting angle of the die channels was 120° . The billets were treated by 6 passes.

Table 1. Chemical composition of AZ91 magnesium alloy, wt. %.

elements	Al	Zn	Mn	Si	Fe	Be	Ni	Cu	Mg
wt. %	8.7	0.65	0.25	0.006	0.003	0.0008	0.0006	0.0005	rest

The semi-products used for machining of the fatigue specimens were cylindrical rods of 80 mm length and 15 mm in diameter. The specimen geometry is shown in Fig. 1. Gauge length of the specimens was carefully polished for the following inspection with the aim to reveal the development of slip bands and cracks. The procedure of gauge length preparation consisted of mechanical grinding (SiC papers, No. 800, 1200 and 2500) and mechanical polishing ($1\ \mu m$ diamond paste). In some cases also electrolytic polishing or etching before the testing was applied. Due to the reaction of the chemical solutions with the surface the microstructure was visible and the relationship of the structural features and the crack initiation can be examined.

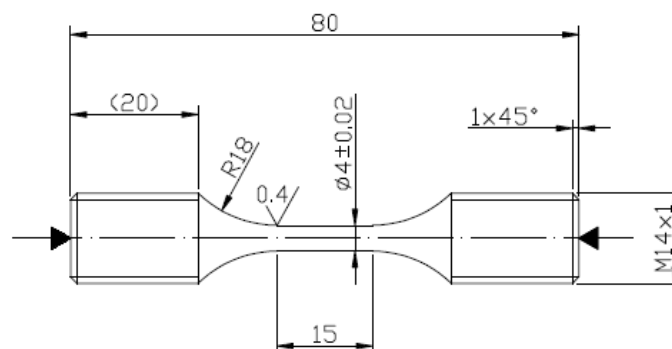


Fig. 1. Fatigue test specimen geometry.

Load controlled cycling in symmetrical tension-compression (load ratio $R = -1$) was used for fatigue testing in the Shimadzu EHF-F1 servo-hydraulic system. The loading frequency was in the range 0.1 to 10 Hz in the low-cycle fatigue region. When the specimen lifetime exceeded 1×10^6 cycles, the specimen was moved to the Amsler HFP 5100 resonant fatigue

machine and the loading was continued with a frequency of about 60 Hz. Tests were conducted at room temperature in laboratory air.

Tescan LYRA 3 XMU FEG/SEM x FIB scanning electron microscope (SEM) was used for observation and analysis of microstructure and the examination of specimen gauge length surface after fatigue tests. Focused ion beam (FIB) technique was applied to examine the characteristic features of microstructure and formation of surface relief and early cracks.

3. Results and discussion

3.1. Structure

The structure of cast specimens consists of solid solution of alloying elements in magnesium, eutectic (solid solution of alloying elements in magnesium + $Mg_{17}Al_{12}$ particles) and discontinuous precipitates and intermetallic particles. The solid solution consists of grains with the average grain size of $185 \pm 70 \mu\text{m}$. The characteristic structure of AZ91 in cast state is shown in Fig. 2a.

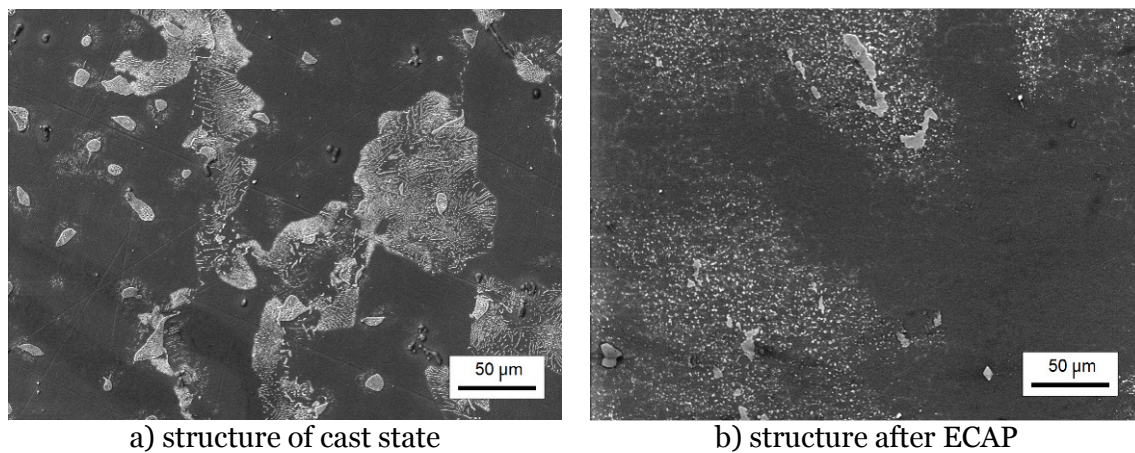


Fig. 2. Characteristic structure of AZ91 magnesium alloy, etched by Nital, SEM.

The structure of specimens treated by 6 passes of ECAP consists of grains of solid solution of alloying elements in magnesium, $Mg_{17}Al_{12}$ intermetallic particles and AlMn based intermetallic particles. The structure can be characterized as bimodal from the macroscopic point of view. There are areas with small grains there with the average grain size of $3.3 \pm 0.5 \mu\text{m}$ with large amount of small $Mg_{17}Al_{12}$ particles. Besides these fine grained areas there are also areas with larger grains, with the average grain size of $9.9 \pm 4.5 \mu\text{m}$ where the density of small $Mg_{17}Al_{12}$ particles is markedly lower. A typical example of the bimodal structure of AZ91 after ECAP is shown in Fig. 2b. It can be seen that some amount of large primary $Mg_{17}Al_{12}$ particles and AlMn based intermetallic particles remained in the ECAPed structure.

The observed bimodality of structure after ECAP can be explained by missing heat pretreatment of cast material before ECAP. According to the observation by Chen et al. [15] the microstructure of AZ91 magnesium alloy after ECAP looks to be strongly influenced by the structure before ECAP treatment. When the heat pretreatment is optimal, the ECAP results in creation of fine grained structure as early as after 2 passes. Following passes cause only homogenization of the structure, without any important influence on the grain size. In the case of missing heat pretreatment the structure obtained after 6 passes can remain bimodal as in the present study. Simultaneously, the tensile properties and ductility of bimodal structure are substantially improved when compared to the cast state [5, 7, 8, 13].

3.2. S-N curves of cast and ECAPed material

The experimentally determined S-N curves in Fig. 3 show improvement of fatigue properties of AZ91 magnesium alloy processed by ECAP treatment.

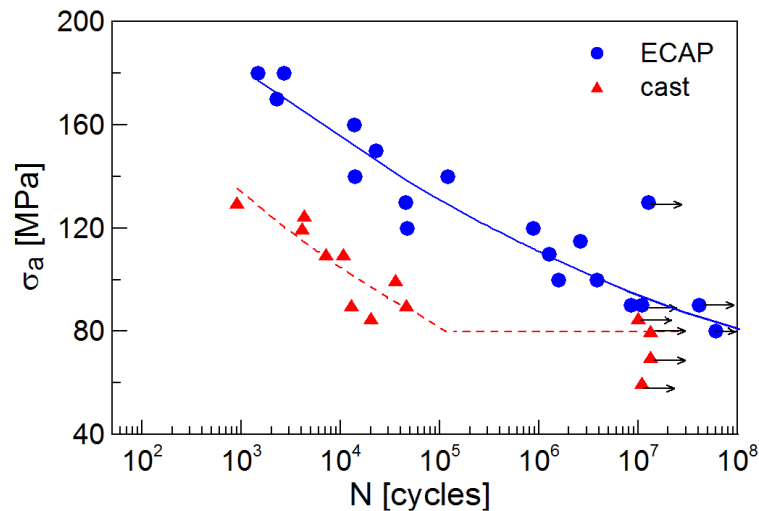


Fig. 3. Fatigue test results.

The S-N curve of cast AZ91 exhibits a typical knee. All the specimens tested at higher stress amplitudes than 80 MPa failed before they reached 10^5 cycles. Specimens tested at the stress amplitudes below 80 MPa exceeded 10^7 cycles without failure. They were considered run-outs and the corresponding points are denoted by arrows in the Fig. 3.

Specimens machined from ECAPed billets tested at same stress amplitudes as specimens manufactured from the cast material exhibit higher number of cycles to the failure. The S-N curve of ECAPed material is shifted by two orders of magnitude towards higher lifetimes in comparison with the as-cast state. The curve does not exhibit the knee in the investigated interval of the stress amplitudes and number of cycles to failure. The fatigue life continuously increases with decreasing stress amplitude and meets the horizontal part of the S-N curve of the cast material in the region of 10^7 to 10^8 cycles. The experimental results clearly indicate that the ECAP of cast AZ91 does not bring a benefit as regards the high cycle fatigue strength.

3.3. Crack initiation

In both states of examined material the solid solution areas are the more ductile constituents where the cyclic plastic deformation takes place. The eutectic and large $Mg_{17}Al_{12}$ and AlMn based intermetallic particles are substantially harder constituents of the structure.

In the cast material the slip band formation was observed on the specimen surface in the areas of solid solution. The length of the bands is limited by the dimension of areas of solid solution, Fig. 4a. No slip bands were observed in the eutectic. The cracks initiate on the long well developed slip bands, often inclined at the angle of 45° to the loading axis. The cracks develop lengthwise the slip bands and often exhibit remarkable opening. Later on the cracks tend to grow perpendicularly to the loading axis. When the brittle constituents are present in the crack trail they fail by brittle manner or the crack grows through the interface of the solid solution and the hard particle, due to concentration of stress ahead of the crack tip. These observations are in agreement with Wolf et al [14] who observed the crack initiation on slip bands formed in the solid solution areas and on structural defects which were present in their material. In the material examined in this study no internal defects related to the crack initiation were found. It was observed that with decreasing stress amplitude, the count of slip bands drops very quickly. Below 85 MPa no slip bands on the polished and etched specimen

gauge length were observed even after 10^7 cycles. Thus the stress amplitude 85 MPa can be considered a threshold for slip band formation in as cast structure.

In the material after ECAP the mechanism of the fatigue crack initiation in the large grain areas of the bimodal structure (grain size about $10\ \mu\text{m}$) was found to be qualitatively the same as observed in the cast material. The grains formed by solid solution with low density of $\text{Mg}_{17}\text{Al}_{12}$ particles were predominant places of slip band formation, Fig. 4b. The slip bands are, due to small grain size, much shorter than in the cast material. Also the distance between parallel slip bands in the ECAPed material is smaller. The whole process is substantially scaled down when compared to the cast state. Also the transition to the crack propagation perpendicularly to the loading axis starts much earlier, i.e. for quite short cracks developed in slip bands. This is shown in Fig. 4b, where the cracks macroscopically propagate perpendicularly to the loading axis (marked by arrows in Fig. 4b). The crack initiation in a slip band requires a definite amount of cyclic plasticity to produce the necessary material damage. This is in agreement with observations of Chung et al. [8]. It is obvious, that the crack initiation and early crack growth in a fine grained structure are more difficult than in the coarse grained case due to higher number of barriers.

Similarly to the cast state, with decreasing stress amplitude the number of slip bands rapidly decreases. The multiple crack initiation ceases quickly and single crack initiation becomes decisive. Below 120 MPa no slip bands on the polished and etched specimen gauge lengths were observed. Consequently, this stress amplitude can be considered a threshold for formation of the slip bands in the fine-grained structure. Simultaneously, the stress amplitude 130 MPa is a level, at which a run-out specimen was found, Fig. 3. Nevertheless, some specimens failed also below this stress level. This means that at least one crack had to initiate on the specimen gauge length and this crack caused the fatigue failure. Detailed inspection of the fracture surfaces of specimens which failed below 130 MPa together with observation of microstructure gave evidence that the initiation took place in the large grained area.

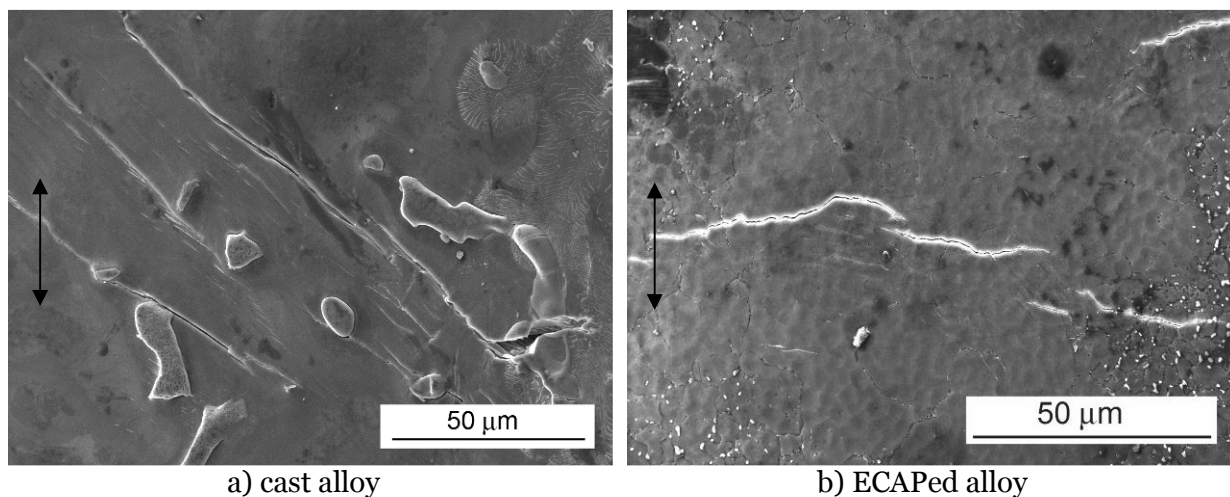


Fig. 4. Slip bands and fatigue cracks on the specimen surface after fatigue loading.

Results of the examination of the surface relief and microstructure in the vicinity of early cracks by FIB are shown in Fig. 5 and 6. A set of slip bands in cast material can be seen in Fig. 5a. This set was covered by protective platinum layer for the FIB cutting and following surface relief observation. Fig. 5b documents high extrusions above the plain surface which correspond to the slip bands visible in the Fig. 5a. Intrusions are inexpressive; however material damage along the straight slip planes below them can be seen. In the case of long slip bands the well developed straight cracks along these planes are visible. The initiation of

fatigue cracks in Mg alloys is often described in literature as quasi-cleavage [16], without detailed description of the inherent mechanism. The existence of well-developed extrusions witnesses for severe concentration of the cyclic plasticity and slip activity within the slip bands. From this aspect the mechanism of crack initiation resembles that known from f.c.c. metals.

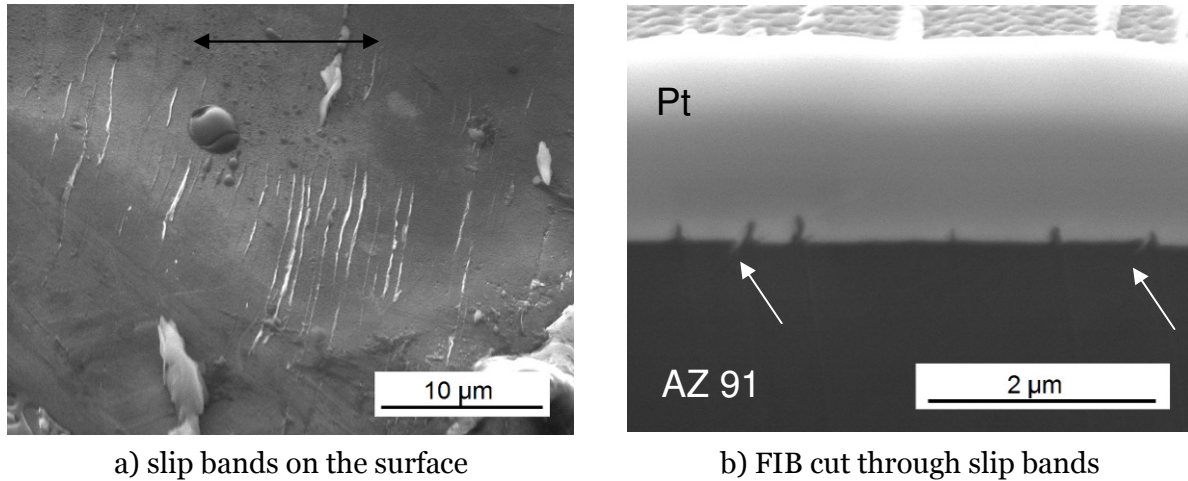


Fig. 5. Slip bands in cast alloy, specimen tested at $\sigma_a = 120$ MPa, $N_f = 4\ 088$ cycles.

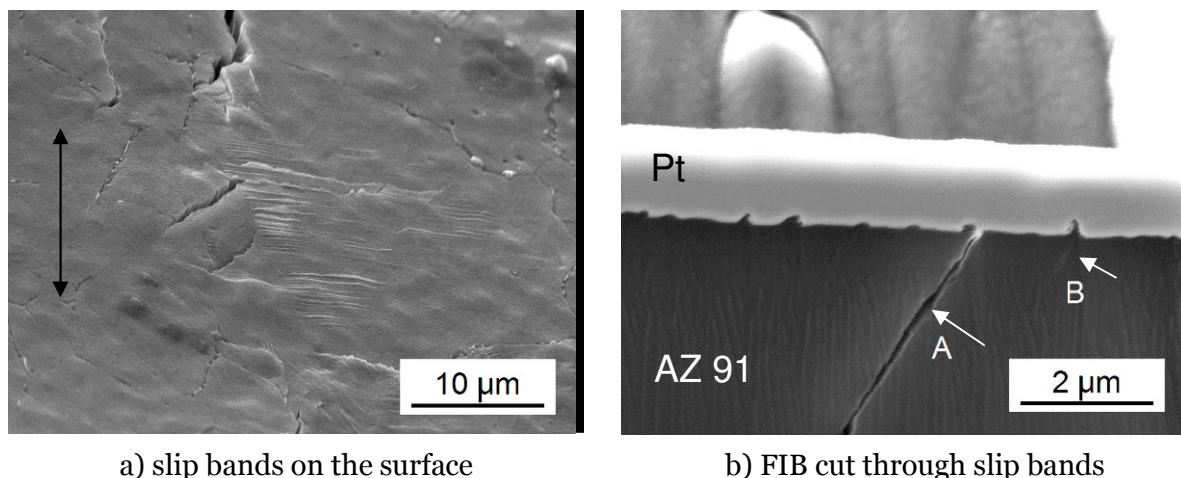
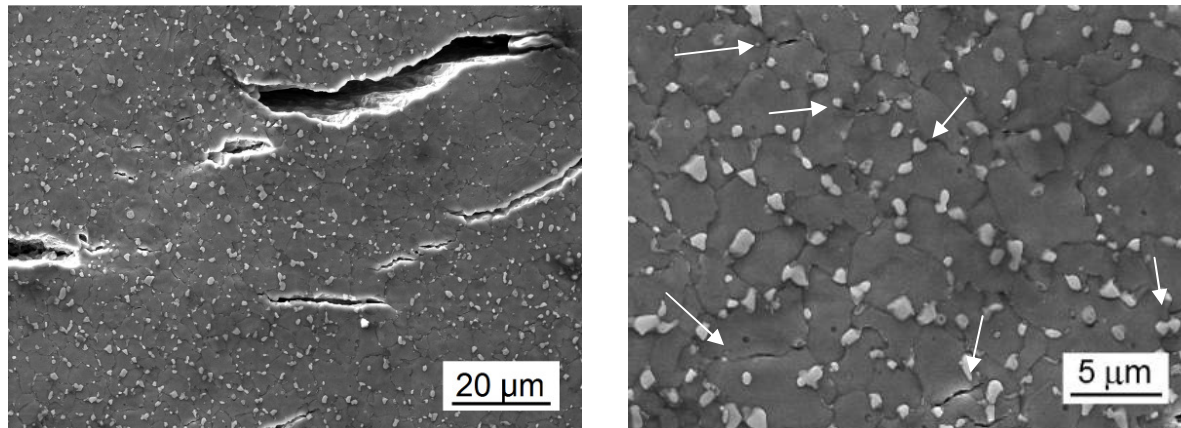


Fig. 6. Slip bands in alloy after ECAP, specimen tested at $\sigma_a = 180$ MPa, $N_f = 1\ 473$ cycles.

An example of the surface of large grained area of the bimodal structure after fatigue loading can be seen in Fig. 6a. The slip bands with clear extrusions appear only in suitably oriented grains, whereas neighboring grains does not exhibit any apparent slip activity in terms of slip band formation. Fig. 6b shows the FIB cut perpendicular to the surface and nearly perpendicular to the slip bands. Similarly to the cast material the extrusion profile is visible on the surface. Some of extrusions are related to cracks. The crack denoted by A is well developed, running crystallographically along the slip plane into material interior. The fracture surfaces are clearly separated and the crack runs across the whole grain. The crack denoted by B, which is also related to the extrusion on the surface is short (about 1 μm) and does not represent fully separated material. It is worthwhile to mention that there seems not to be any relation between the height of extrusions and the length of a related crack.

From Fig. 6a it is evident that besides the slip bands, grain boundary cracks appear in the structure. An example of this type of cracking in fine grained area is shown in Fig. 7. In the

neighbouring grains no apparent signs of cyclic plasticity in terms of slip bands can be detected. This type of crack initiation was not observed in the cast material.



a) cracks in area with small grains

b) detail of grain boundary cracks

Fig. 7. Grain boundary cracks in alloy after ECAP, specimen tested at $\sigma_a = 180$ MPa, $N_f = 1\,473$ cycles.

3.4. Fatigue life

ECAP treatment obviously improves fatigue strength in the low-cycle fatigue region. This effect is related to substantially higher σ_{UTS} and $\sigma_{0.2}$ of the alloy after SPD treatment, which is connected with microstructural changes and strengthening due to the ECAP [5, 13]. However, no significant difference in the endurance limit based on 10^7 cycles of the cast alloy and the alloy after ECAP follows from the experimental data shown in Fig. 3. For both tested material states, similar stress amplitude can be considered as the endurance limit; 80 MPa for as-cast state and 90 MPa for ECAPed alloy. The value for cast material corresponds well with the average value of the endurance limit 80 - 90 MPa of cast AZ91 alloy based on large set of literature data [1]. Simultaneously this amplitude is the threshold amplitude for development of slip bands which are sites of initiation of fatigue cracks. In material processed by ECAP the development of slip bands which are responsible for initiation of fatigue cracks ceases when the stress amplitude decreases below 120 MPa. However, due to the existence of simultaneous crack initiation mechanism related to the grain boundary cracking the endurance limit further decreases. The number of experimental S-N points presented in Fig. 3 in the region of endurance limit is not very high. It would be worthwhile to determine experimentally the endurance limit for ECAPed material by stair case method and to evaluate statistically the scatter of data for both states of material. However, this task is beyond the range of this work.

4. Conclusions

- ECAP treatment improves the fatigue strength of AZ91 alloy. The S-N curve is shifted by two orders of magnitude towards higher number of cycles to failure when compared to the cast alloy. The endurance limit for 10^7 cycles of cast and ECAPed alloy is nearly the same.
- Two types of the fatigue crack initiation were observed. In the cast material the cracks initiate exclusively in the cyclic slip bands. They are formed in solid solution areas with low density of $Mg_{17}Al_{12}$ particles. In the alloy processed by ECAP identical mechanism operates, however due to small grain size the lengths of slip bands in which cracks develop is substantially smaller. Besides initiation in slip bands grain boundary cracking was observed in ECAPed alloy.

Acknowledgments

The Czech Science Foundation under the contract 108/10/2001 and Ministry of Education of the Czech Republic under the project CZ.1.07/2.3.00/30.0039 supported this work.

References

- [1] Altwicker H et al 1939 *Magnesium und seine Legierungen* (Berlin: J. Springer Verlag)
- [2] Němcová A et al 2009 *Mat. Eng.* **16** (4) pp 5-10
- [3] Bukovina M, Škorík V, Hadzima B *Proc. TRANSCOM 2009* (University of Žilina) pp 37-42.
- [4] Eisenmeier G 2001 *Mat. Sci. and Eng. A* **319-321** pp 578-582
- [5] Chung C W et al 2010 *J. Phys.: Conf. Ser.* **241** 012101
- [6] Ebel-Wolf B, Walther F, Eifler D 2008 *Mat. Sci. and Eng. A* **486** pp 634-640
- [7] Yamashita A, Horita Z, Langdon T G 2001 *Mater. Sci. and Eng. A* **300** pp 142-147
- [8] Chung C W et al 2009 *IOP Conf. Series: Mat. Sci. and Eng.* **4** doi:10.1088/1757-899X/4/1/012012
- [9] Chen B et al 2008 *Mat. Sci. Eng. A* **483-484** pp 113-116
- [10] Chung Ch S, Chun D K, Kim H K 2005 *J. of Mech. Sci. and Technol.* **7** pp 1441-1448
- [11] Kim H K, Lee Y I, Chung Ch S 2005 *Scripta Mater.* **52** pp 473-477
- [12] Zúberová Z et al 2007 *Met. Mat. Trans.* **38A** pp 1934-1940
- [13] Chen B et al 2008 *Mat. Sci. and Eng. A* **483-484** pp 113-116
- [14] Wolf B, Fleck C, Eifler D 2004 *Int. J. Fat* **26** pp 1357-1363
- [15] Chen B et al 2008 *Mat. Sci. and Eng. A* **483-484** pp 113-116
- [16] *Fatigue and Fracture* 1996 ASTM Handbook vol.19 (ASTM Int. Materials Park, OH., U.S.A.) p.875.